



Fermi National Accelerator Laboratory

FERMILAB-Pub-80/96-EXP
7420.180
(Submitted to Nucl. Phys. B)

QUARK JETS FROM ANTINEUTRINO INTERACTIONS II INCLUSIVE PARTICLE SPECTRA AND MULTIPLICITIES IN THE QUARK JETS

V. V. Ammosov, A. G. Denisov, G. S. Gapienko,
V. A. Gapienko, V. I. Klukhin, V. I. Koreshev,
P. V. Pitukhin, V. I. Sirotenko, E. A. Slobodyuk,
Z. V. Usubov, and V. G. Zaetz
Institute of High Energy Physics, Serpukhov, USSR

and

J. P. Berge, D. Bogert, R. Endorf,* R. Hanft,
J. A. Malko, F. A. Nezrick, and R. Orava†
Fermi National Accelerator Laboratory
Batavia, Illinois 60510 USA

and

V. I. Efremenko, A. V. Fedotov, P. A. Gorichev,
V. S. Kaftanov, G. K. Kliger, V. Z. Kolganov,
S. P. Krutchinin, M. A. Kubantsev, I. V. Makhljueva,
V. I. Shekeljan, and V. G. Shevchenko
Institute for Theoretical and Experimental Physics
Moscow, USSR

and

J. Bell, C. T. Coffin, B. P. Roe, and D. Sinclair
University of Michigan
Ann Arbor, Michigan 48104 USA

September 1980

*Visitor from the University of Cincinnati, Cincinnati, Ohio
†On leave from the University of Helsinki, Helsinki, Finland

ABSTRACT

We present results on inclusive particle production in the antineutrino charged current induced hadron jets observed in the Fermilab 15-ft. bubble chamber. Fractional energy distributions, particle ratios and average multiplicities of the hadrons in the jets are measured. Ratios between the inclusive production rates of different mesons in the jets are studied to seek evidence for the d-quark origin of the observed hadrons. Good over-all agreement with the hypothesis of d-quark fragmentation with universal fragmentation functions obeying isospin systematics is established.

1. Introduction

Inclusive single-particle spectra in lepton induced hadron jets can be used to test the quark-parton picture of quark fragmentation as the source of the observed hadron showers. Particles in the jets should appear in ratios which reflect the flavor of the original fragmenting quark.^{1,2,3} Antineutrino (neutrino)-nucleon charged current interactions are particularly suited for these tests because of the theoretical possibility of choosing the fragmenting quark flavor to be "down" ("up").

In this article we will investigate single hadron distributions in the current fragmentation region of deeply inelastic antineutrino-nucleon charged current interactions. We have earlier reported our studies on the jet net charge and factorization properties of the single particle cross-section in the antineutrino induced jets.^{2*} This analysis serves as a direct continuation to our search for evidence of the d-quark origin of the hadron showers produced in antineutrino-nucleon interactions.

In a forthcoming paper⁵ we will report our detailed studies on the transverse structure of the antineutrino charged current induced jets.

2. Experimental details

The experimental data come from a wide-band antineutrino exposure of the Fermilab 15-ft. bubble chamber filled with a heavy neon-hydrogen mixture. From the total of 23,000 neutral particle induced events which have been fully measured, we have chosen 7200 charged current antineutrino events. The

selected event sample fulfils the following criteria: (1) the incident antineutrino energy is larger than 10 GeV; (2) each event contains a positively charged muon identified by the External Muon Identifier supplemented by a kinematical method of identification; (3) The laboratory momentum of the muon is required to be larger than 4 GeV/c.

Multiplicity dependent weights are assigned to all events to account for the scanning inefficiencies (35% for the two-pronged events, 1% for the six- and higher-pronged events). A weighting procedure is also applied to all secondary tracks to account for the interactions occurring close to the main interaction point. This momentum dependent weight has an average value of 1.09.

In this analysis, we shall exclude all identified protons and assign the pion mass to all remaining particles. The uncertainties arising from this procedure as well as the uncertainty caused by the energy reconstruction procedure are studied separately for each inclusive spectrum. The fractional energy distribution of the positively charged mesons is obtained by correcting for the unidentified protons via the observed spectrum of lambda-hyperons. Details of this procedure are given in the Appendix. The total contribution from protons in the current fragmentation region, with the selection $W > 3$ GeV, relative to all positively charged hadrons is $(15 \pm 3)\%$.

Energy smearing of the distributions is accounted for by calculating the ratios $D(z)^{\text{unsmeared}}/D(z)^{\text{smeared}}$ from a Monte

Monte Carlo model.⁶ This Monte Carlo model includes the measurement systematics, nuclear Fermi motion and the initial antineutrino energy spectrum. The net effect of the energy smearing, varies from 5% at small z-values to 15% at the highest values of z ($z \leq 0.8$). Further details on the experiment and the selection procedure for the current fragments are given in Ref. 4. Details concerning the sample of neutral strange particles used in this analysis are given in Ref. 7.

3. Single-particle distributions

The factorization hypothesis for the differential cross section

$$\frac{d^2\sigma}{dx dz} = \frac{G^2 M E \bar{\nu}}{\pi} \sum_i f_i(x_B) D_i^h(z)$$

where $f_i(x_B)$ are the nucleon structure functions and $D_i^h(z)$ are the fragmentation functions for parton i into hadron h , is well satisfied at present energies for the final state hadrons in the current fragmentation region.⁸ The variables x_B and z are defined in the laboratory system as $x_B = -q^2/2M\nu$, and $z = E_h/\nu$, where M is the nucleon mass, $\nu = E_{\bar{\nu}} - E_{\mu}$, $-q^2$ is the lepton four-momentum transfer squared, $E_{\bar{\nu}}$, E_{μ} and E_h are the energies of the incident antineutrino, final state muon and final state hadron, respectively. We define the fragmentation function as $D_i^h(z) = (1/N_{ev}) (dN^{\text{tracks}}/dz)$, where N_{ev} and N^{tracks} are the numbers of events and number of tracks of type h , respectively.

We shall consider only particles travelling forward in the hadronic center-of-mass system (current fragmentation region). To ensure adequate separation between the current and target fragmentation regions we shall select the center-of-mass energies, W , larger than 3 GeV, and the current four-momentum squared, $-q^2$, larger than $1 \text{ GeV}^2/c^2$.

In the antineutrino-nucleon charged current interactions one effectively selects the fragmenting quark flavor to be d for $x_B > 0.1$.⁴ Most of the fragmentation products are pions (90%)⁵ and therefore, using the isospin symmetry, the relation $D_d^{h^\pm}(z) \simeq D_u^{h^\pm}(z)$ is expected to be valid.

It follows from isospin conservation that for any quark i the relation $D_i^{\pi^+}(z) + D_i^{\pi^-}(z) = 2 D_i^{\pi^0}(z)$ holds. We test this relation in Fig. 1 where the fragmentation function $D^{h^+} + D^{h^-}$ is plotted together with the data for $2 D^{\pi^0}(z)$ from an electroproduction experiment.⁶ Good agreement between our antineutrino interaction data and the electroproduction data is observed. In the same figure also e^+e^- annihilation results,⁷ electroproduction data for charged hadrons⁸ and proton-proton data¹⁰ for charged hadrons are shown. The agreement of the different data sets for $D^h(z)$ supports the QPM expectation of the universal quark fragmentation functions. The isospin symmetry in the quark jets also implies that $D_u^{\pi^-}(z) = D_d^{\pi^+}(z)$ and $D_u^{\pi^+}(z) = D_d^{\pi^-}(z)$. We test these equalities in Fig. 2 and 3 where $D_d^{h^\pm}(z)$ and $D_u^{h^\pm}(z)$ are plotted for our antineutrino charged current events and for neutrino-proton charged current events. Recent data from a $\bar{\nu}p$ experiment at Fermilab is also shown in Fig. 2 and 3.¹⁶ The

agreement between $D_d^{h^+}(z)$ and $D_u^{h^-}(z)$ supports the quark origin of the observed hadrons in the current fragmentation region. Fig. 3 on the other hand, demonstrates the importance of the proton correction: the difference between our measurement for $D_d^{h^-}(z)$ and a measurement for $D_u^{h^+}(z)$ is most probably due to the proton contamination in $D_u^{h^+}(z)$.

Fragmentation functions for the K^0 -mesons, $D^{K^0}(z)$, and lambda-hyperons $D^\Lambda(z)$, are shown in Fig. 4.

The experimental data are compared with the QPM parametrizations of Field and Feynman. For these predictions we have used the analytical approximations given in Ref. 11 with the SU(3) symmetry violation parameter of 0.27 ± 0.04 measured in this experiment.³

The fragmentation functions evaluated for our anti-neutrino induced charged current jets give support for the two fundamental hypotheses of the quark-parton model: (1) Universality of the quark hadronization process, and (2) systematic isospin relations between d and u quark jets.

4. Particle ratios

The ratio of π^- to π^+ mesons produced in $\bar{\nu}_\mu N$ charged current interactions at the current interactions at the limit $z \rightarrow 1$ should directly measure the ratio between the initial quark flavors d to u. For antineutrino charged current interactions this prediction means that the ratio π^-/π^+ should approach infinity as z approaches unity.¹¹

Since we do not generally identify charged kaons in our sample of secondary particles we consider the ratio h^-/h^+ between the charged hadrons in the current fragmentation

region. In Fig. 5 we show the ratio $h^-/h^+ = D^{h^-}(z)/D^{h^+}(z)$ as a function of z .

The ratio is seen to increase with increasing z . We compare our experimental data to the QPM prediction obtained from the Field and Feynman parametrizations for the $D_d^{h^\pm}(z)$ -functions. The prediction shown in Fig. 5 is calculated from the analytical expression given in Ref. 11 for the fragmentation functions $D_d^{h^\pm}(z)$ with the SU(3) symmetry violation parameter of 0.27 as measured in this experiment.³ The pseudoscalar to vector meson production rates are assumed to be equal to each other. The prediction agrees well with the experimental data.

To check for possible threshold behavior in the ratio we have plotted h^-/h^+ as a function of W^2 in Fig. 6a. No significant variation with W^2 is observed. In Fig. 6b we have plotted h^-/h^+ as a function of $-q^2$. No apparent dependence of the ratio on $-q^2$ is seen. The quark fragmentation model requires the constancy of the h^-/h^+ -ratio with respect to the Bjorken- x variable. Due to the isospin symmetry $D_u^{h^\pm}(z) \sim D_d^{h^\pm}(z)$ the ratio should also be constant in the small x_B -region ($x_B < 0.1$), where the quark-antiquark sea dominates. In Fig. 6c we show the ratio h^-/h^+ as a function of x_B . No significant variation with x_B is observed in accordance with the QPM expectation. Finally, possible resonance production effects should show up when the ratio h^-/h^+ is plotted as a function of the transverse momentum with respect to the jet axis, p_{\perp} . However, no variation is observed (Fig. 6d).

Measurement of the ratio $h^-/h^+ = D^{h^+}(z)/D^{h^-}(z)$ therefore supports the QPM prediction that the d-quark "hadronization" is the origin of the mesons observed in the current fragmentation region in $\bar{\nu}_\mu N$ charged current interactions.

5. Jet Multiplicities

Charged particle multiplicities in the current induced jets provide a powerful tool for testing various theoretical models. Parametrization of the jet multiplicities is also essential for reliable predictions needed for more energetic quark jets produced with forthcoming accelerators.

The average charged particle multiplicity is observed to grow logarithmically as a function of the jet energy up to $W = 10$ GeV in all hard scattering processes. Recent data on e^+e^- -annihilation above 10 GeV c.m.s energies shows, however, a rapid increase of the jet multiplicities.⁹ The increase can be fitted well with a power law $\langle n \rangle_{\text{jet}} \propto W^{1/2}$ or with a QCD-based parametrization $\langle n \rangle_{\text{jet}} = \exp(2\sqrt{n_c/\pi b}(\ln(W^2/\Lambda^2)))$, where $b = (11 - 2n_f/3)/4\pi$, Λ is the scale parameter ($\Lambda \leq 0.5$ GeV), n_f is the number of quark flavors and n_c is the number of colors ($n_c = 3$).¹²

In Fig. 7a we show the average charged particle multiplicity in the antineutrino charged current induced jets as a function of the c.m.s energy squared. The data can be fitted well with all the expressions discussed above. The parameterizations obtained follow,

$$\langle N \rangle_{\text{jet}} = A + B \ln W^2 + C (\ln W^2)^2$$

with $A = -(2.04 \pm 1.06)$, $B = (1.75 \pm 0.67)$, and $C = -(0.13 \pm 0.10)$;
for a power-law

$$\langle n \rangle_{\text{jet}} = A + B W^{1/2}$$

$A = -(1.35 \pm 0.29)$, $B = (1.55 \pm 0.14)$, and for the QCD
expression

$$\langle n \rangle_{\text{jet}} = A + B \exp(b' (\ln(W^2/\Lambda^2))^{1/2})$$

where $b' = 2 \sqrt{\frac{n_c}{\pi b}}$, $A = 1.66 \pm 0.05$, and $B = (0.78 \pm 0.09) \times 10^{-2}$.

A comparison of these results with the e^+e^- data⁹
(Fig. 7) shows agreement when the e^+e^- data are
multiplied by a factor of two to account for the two jets
observed in the e^+e^- final states.

In Fig. 8 the average jet multiplicity is plotted as a
function of $-q^2$ for fixed W -intervals. No significant $-q^2$ -
dependence is observed in accordance with Bjorken
correspondence principle.¹³ Similarly, Fig. 9a shows the x_B
dependence of $\langle n \rangle_{\text{jet}}$ and Fig. 9b the x_B -dependence with fixed
 W . No apparent x_B -dependence is seen.

To study possible two-particle correlations in the anti-neutrino charged current induced jets we plot in Fig. 10 the integrated two-particle correlation parameter

$$f_2 = \langle n(n-1) \rangle - \langle n \rangle^2 = D^2 - \langle n \rangle$$

where D is the dispersion of the multiplicity distribution, $D = \sqrt{\langle n^2 \rangle - \langle n \rangle^2}$, and f_2^{++} , f_2^{--} , f_2^{+-} are defined for the positively charged, for the negatively charged and for all charged final state particles in the jets, respectively. A linear decrease of the f_2^{--} -parameter as a function of $\langle n \rangle$ is seen. This behavior is expected in models which are based on the multiperipheral type of particle production, where short range correlations dominate amongst the final state particles. The correlation parameter f_2^{++} seems to stay constant as a function of $\langle n \rangle$.

A way to combine the above observations is to use the Koba-Nielsen-Olesen (KNO-) scaling representation.¹⁴ In this representation the partial cross section is multiplied by $\langle n \rangle$ and plotted as a function of the scaled multiplicity $n/\langle n \rangle$. Fig. 11 shows the first KNO-scaling results for the lepto-produced jets. The multiplicity distributions are evaluated in different W -intervals and plotted in the same figure. Resulting scaling distributions for our antineutrino-nucleon interactions and for two hadron-hadron experiments¹⁵ are shown in this same figure. The antineutrino charged current induced jets give rise to a scaling distribution which is significantly narrower than that for the hadron-hadron forward multiplicities. The antineutrino data give, on the other

hand, significantly narrower distribution than purely statistical particle correlations would indicate (for Poisson distribution $f_2 \equiv 0$). This behavior was already observed with the two-particle correlation parameters, f_2 , and it is typical for short range correlations amongst the final state hadrons.

6. Conclusions

We have measured the quark fragmentation functions $D^{h^+}(z)$, $D^{h^-}(z)$, $D^{K^0}(z)$ and $D^\Lambda(z)$ in the $\bar{\nu}_\mu N$ charged current interactions. Universal fragmentation functions are seen to result from deeply inelastic lepton-nucleon interactions, from e^+e^- -annihilations and from recent proton-proton data from the ISR-experiments.

The isospin systematics implied by the simple QPM are found to be valid for the fragmentation functions measured in our experiment.

The ratio h^-/h^+ supports the cascade picture of quark fragmentation and provides evidence for the d-quark origin of the observed hadron jets.

Charged hadron multiplicities are evaluated in the $\bar{\nu}_\mu N$ charged current jets and useful parametrizations for the jet multiplicities are provided. The antineutrino produced jets are found to resemble those produced in e^+e^- annihilation to hadrons.

Acknowledgements

We thank Kenneth Lassila for discussions.

APPENDIX

**CORRECTION PROCEDURE FOR PROTON BACKGROUNDS
IN POSITIVE MESON DISTRIBUTIONS.**

QUARK JETS II

APPENDIX A

Correction Procedure for Proton Background in Positive Meson Inclusive Distributions.

In order to study the inclusive particle distributions of positively charged mesons one must be able to subtract the contribution of protons. The difficulty in high energy bubble chamber experiments is that only protons with laboratory momenta less than $\sqrt{1}$ GeV/c can be distinguished from positively charged mesons. All positive tracks of momenta > 1 GeV/c are included and assigned a pion mass. The unidentified protons, when assigned the pion mass and Lorentz - transformed into the hadronic center-of-mass system (c.m.s), are shifted towards the forward c.m.s. hemisphere.

We have indirectly calculated the contribution of the unidentified protons by utilizing the distributions of the lambda-hyperons observed in this experiment. The Quark Parton Model of hadron production in deep inelastic scattering relates the production rates of strange and non-strange mesons by the amount of SU(3) symmetry violation in the quark jet cascade. We assume that a straightforward extension of this picture holds for the production rates of strange and non-strange baryons above the kinematic thresholds. Since a lambda differs from a proton only in the replacement of an s-quark in the lambda by a u-quark, the only difference between the distributions of lambdas and protons in the model is the normalization, which is given by the amount

of $SU(3)$ symmetry violation in the quark jets. This procedure for the calculation of the inclusive distribution of protons is experimentally supported by the observation that the fractional energy distribution of the lambdas in our anti-neutrino charged current interactions and that of the protons reported in an electroproduction experiment have the same shape. ⁷

The fractional energy distribution of all lambdas traveling forward in the hadronic c.m.s. is shown by the solid points in Fig. A1. The lambdas in this distribution have been weighted to correct for escape probabilities, unseen decay modes and smearing of the distribution due to the energy reconstruction procedure. A detailed discussion of the lambda selection and weighting procedure can be found in Ref. 7. When assigned the pion mass, the Lorentz-transformation of all lambdas to the hadronic c.m.s. results in a sizable contamination of target fragments in the current fragmentation region. To study the effect of unidentified protons, the fractional energy distribution of forward traveling lambdas with momenta > 1 GeV/c is plotted (open circles) in Fig. A1, where we have used the pion mass rather than the lambda mass. This sample of lambdas, which has been chosen to simulate the unidentified protons, dominates the low z region ($z < 0.3$). In the higher z region ($z > 0.3$) the contribution of this "unidentified proton" sample of lambdas is found to be about the same as the true sample of lambdas.

The uncorrected fractional energy distribution in the current fragmentation region shown in Fig. 2 is for all positively charged hadrons to which the pion mass was assigned with only identified protons ($P_{lab} < 1$ GeV/c) excluded. Also

shown in Fig. 2 is the corrected distribution obtained by subtracting the distribution of the unidentified protons, as given by the distribution of the "unidentified proton" lambda sample in Fig. A1. The normalization for the unidentified proton distribution was calculated from the "unidentified proton" lambda sample by using the SU(3) violating parameter $p_s/p = 0.27 \pm 0.04$ measured in the experiment³, where p_s and p are the relative probabilities of finding a strange or a non-strange quark in a quark jet. We calculate that the contribution of protons in the current fragmentation region is $(15 \pm 3)\%$ of the positively charged hadrons. This background consists primarily of protons which belong to the target fragmentation region, but due to their being assigned a pion mass are shifted into the current fragmentation region. The relative contribution of protons which truly belong to the current fragmentation region is $(4 \pm 1)\%$. In the region $z > 0.3$ (where the mass of the particle has less importance) $(20 \pm 6)\%$ of the positively charged hadrons are found to be protons. This value is in good agreement with an electro-production experiment which directly measured the proton z -distribution.

For comparison, we have plotted in Fig. 2 the fractional energy distribution for positive hadrons from antineutrino-Hydrogen interactions and for negative hadrons from neutrino-Hydrogen interactions. We observe that our uncorrected distribution is in good agreement with the positive hadron fractional energy distribution measured in antineutrino-Hydrogen reactions and that these distributions

lie above the negative hadron fractional energy distribution. However, our corrected positive meson distribution is in good agreement with the negative hadron fractional energy distribution from νp interactions (where protons cannot contribute) and are also in good agreement with the QPM parameterization of Field and Feynman.¹¹ These comparisons add further confirmation that our correction procedure for subtracting protons from the distributions of positively charged hadrons is reliable.

References

1. R.P. Feynman, Photon-hadron interactions (W.A. Benjamin, New York, 1972).
2. J.P. Berge et al., Phys. Lett. 91B, 311 (1980).
3. V.V. Ammosov et al., Phys. Lett. 93B, 210 (1980).
4. J.P. Berge et al., Quark jets from Antineutrino Interactions I, Net Charge and Factorization in the Quark Jets, Fermilab Pub-80/62-EXP, 7420. 180 (1980), to be published in Nucl. Phys. B.
5. V.I. Efremenko et al., Quark Jets from Anti-neutrino Interactions III, Transverse Structure of the Quark Jets, to be published.
6. J. Bell et al., Phys. Rev. D18, 3905 (1978).
7. V.V. Ammosov et al., Nucl. Phys. B162, 205 (1980).
8. T.P. McPharlin et al., Phys. Lett. 90B, 479 (1980).

9. R. Brandelik et al., Phys. Lett. 89B, 418 (1980).
G. Wolf, Rapporteur talk at 1979 EPS Int. Conf. on High Energy Physics, Geneva (1979).
10. M. Basile et al., Phys. Lett. 45B, 5 (1980).
11. R.D. Field and R.P. Feynman, Nucl. Phys. B136, 1(1978).
12. W. Furmanski, R. Petronzio, and S. Pokorski, Nucl. Phys. B155, 253 (1979).
K. Konishi, Rutherford Preprint RL-79-035 T241 (1979).
13. J.D. Bjorken, Hadron final states in deep inelastic processes, International Summer Institute on Theoretical Particle Physics 7th, Hamburg (1975) p. 93, and references cited therein.
14. F. Koba, H.B. Nielsen and P. Olesen, Nucl. Phys. B40, 317 (1972).
15. H. Grassler et al., Nucl. Phys. B90, 461 (1975).
E.G. Boos et al., Physics Scripta 15, 305 (1977).
16. M. Derrick et al., Physics Letters 91B, 470 (1980).
17. J. Blietschau et al., Physics Letters 87B, 281 (1979).

Figure Captions

1. Fragmentation function $D^{h^\pm}(z) = (1/N_{ev}) (dN^\pm/dz)$ for charged hadrons traveling forward in the hadronic c.m.s in this experiment, in an ep-experiment,⁸ in a proton-proton experiment at ISR,¹⁰ and the fragmentation function $D^{h^0}(z) = (1/N_{ev}) (dN^0/dz)$ for neutral pions in the ep-experiment.⁹ The solid line represents a parametrization by Field and Feynman¹¹ with the size of SU(3) symmetry violation equal to 0.27 (See the text).
2. Fragmentation functions $D^{h^+}(z) = (1/N_{ev}) (dN^+/dz)$ for positively charged hadrons traveling forward in the hadronic c.m.s in this experiment without correction for the proton contamination (crosses) and with the correction described in the Appendix (solid circles). The fragmentation function $D^{h^+}(z)$ for an $\bar{v}p$ experiment is not corrected for the protons;¹⁶ the fragmentation function $D^{h^-}(z) = (1/N_{ev}) (dN^-/dz)$ measured in a vp experiment¹⁷ is also shown. The solid line is a parametrization by Field and Feynman¹¹ with the size of SU(3) symmetry violation equal to 0.27 (see the text).
3. Fragmentation functions $D^{h^-}(z) = (1/N_{ev}) (dN^-/dz)$ for negatively charged hadrons traveling forward in the hadronic c.m.s in this experiment, in an $\bar{v}p$ experiment,¹⁶ and $D^{h^+}(z) = (1/N_{ev}) (dN^+/dz)$ for positively charged hadrons in a vp -experiment.¹⁷ The solid line is a parametrization by Field and Feynman¹¹ with the size of the SU(3) symmetry violation equal to 0.27 (see the text).

4. Fragmentation functions $D^{K^0}(z) = (1/N_{e\nu})(dN^{K^0}/dz)$ and $D^{\Lambda}(z) = (1/N_{e\nu})(dN^{\Lambda}/dz)$ measured in this experiment. The solid line represents a Field and Feynman parametrization¹¹ for the fragmentation function $D_d^{K^0}(z)$ with the size of SU(3) symmetry violation equal to 0.27. (See the text).
5. Ratio $h^-/h^+ = D^{h^-}(z)/D^{h^+}(z)$ as a function of $z = E_h/\nu$ for the charged hadrons traveling forward in the hadronic c.m.s in this experiment. The solid line is a parametrization of Field and Feynman¹¹ with the size of SU(3) symmetry violation equal to 0.27 (See the text).
6. Ratio $\langle h^-/h^+ \rangle = (\int D^{h^-}(z)dz)/(\int D^{h^+}(z)dz)$ as a function of (a) c.m.s energy squared, W^2 , (b) lepton four-momentum transfer squared, Q^2 , (c) $x_B = Q^2/2m\nu$, and (d) hadron transverse momentum, squared, p_t^2 .
7. Average charged particle multiplicity, $\langle n_{ch} \rangle$, of the hadrons traveling forward in the hadronic c.m.s as a function of (a) c.m.s energy squared, W^2 and (b) lepton four-momentum transfer squared, Q^2 . The solid line represents a power-law parametrization of the average multiplicity and the dashed line a logarithmic parametrization of the average multiplicity as a function of W^2 . The dash-dotted line represents a fit to the e^+e^- data⁹ with the vertical lines indicating typical uncertainties in the measurements.
8. Average charged multiplicity, $\langle n_{ch} \rangle$, of the hadrons traveling forward in the hadronic c.m.s as a function of Q^2 with fixed W -intervals.

9. Average charged multiplicity, $\langle n_{ch} \rangle$, of the hadrons traveling forward in the hadronic c.m.s as a function of (a) x_B , (b) x_B with fixed W -intervals.
10. Integrated two-particle correlation parameter for hadrons traveling forward in the hadronic c.s.m (a) $f^{+-} = \langle n_{ch}(n_{ch} - 1) \rangle - \langle n_{ch} \rangle^2$ as a function of $\langle n_{ch} \rangle$, and (b) $f_2^{\pm\pm} = \langle n_{\pm}(n_{\pm} - 1) \rangle - \langle n_{\pm} \rangle^2$ as functions of $\langle n_{+} \rangle$ and $\langle n_{-} \rangle$, respectively.
11. KNO-scaling representation of the charged multiplicities for hadrons traveling forward in the hadronic c.m.s: $\langle n_{ch} \rangle P_n$ is plotted against $n_{ch} / \langle n_{ch} \rangle$, where $P_n = \sigma_n / \sigma_{tot}$, for this experiment. The solid line represents a fit to the π^+p -data at 8-16 GeV/c incident π^+ momenta and to the $\bar{p}p$ -data at 22.7 GeV/c incident \bar{p} momentum.¹⁵

Fig. A1: Fractional energy distribution $(1/N_{ev})(dN/dz)$ for the lambda hyperons observed in this experiment (full circles). Open circles represent the fractional energy distribution of the observed lambda-hyperons with the selection $P > 1$ GeV/c in their laboratory momenta, and with their masses replaced by the pion mass.

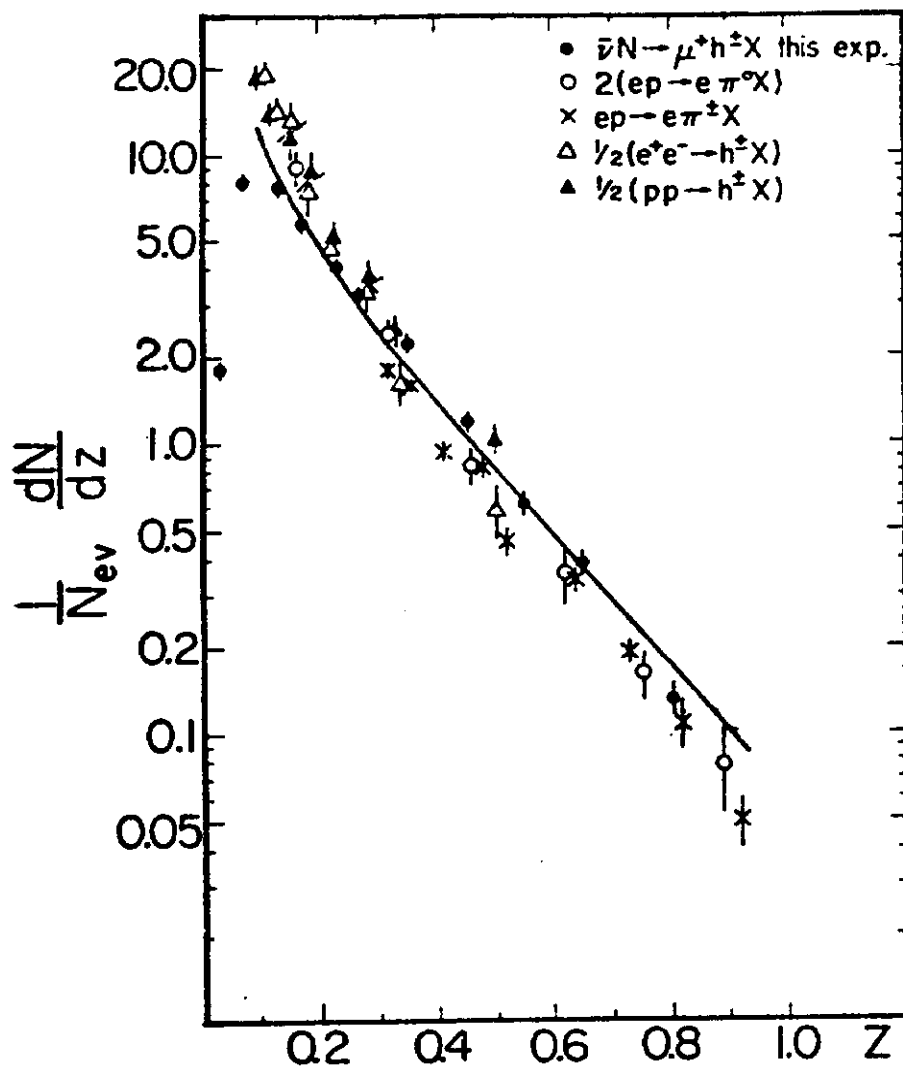


Fig.1

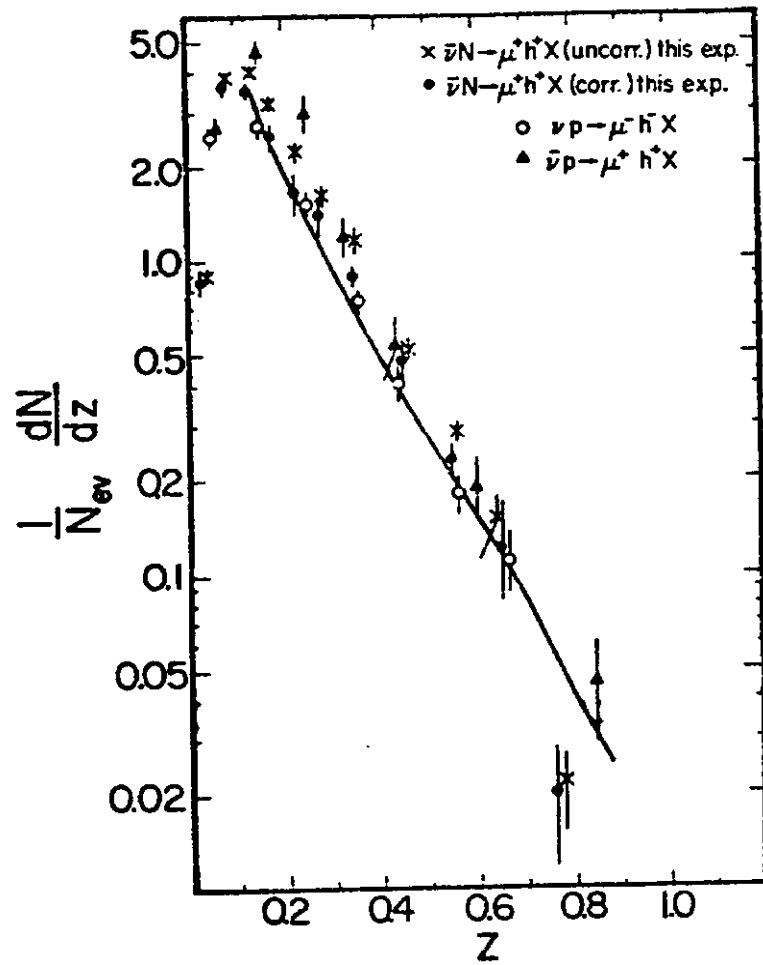


Fig.2

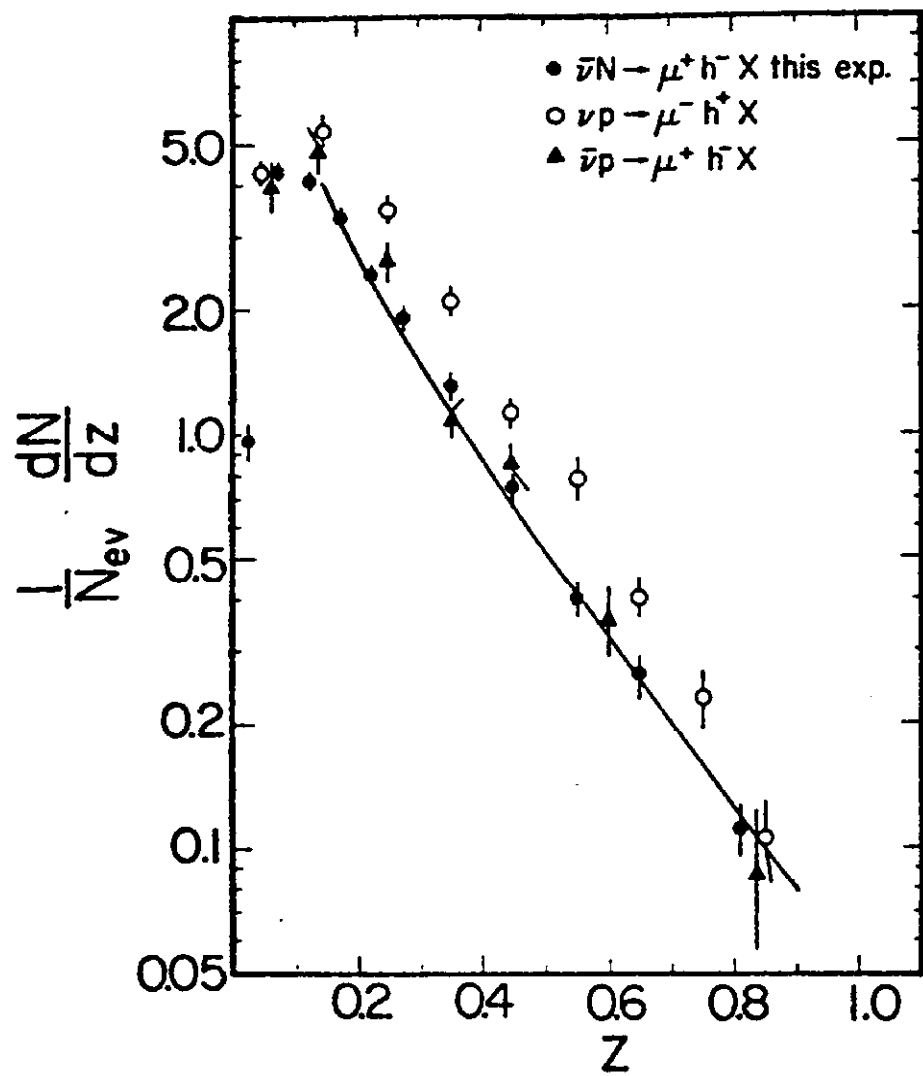


Fig. 3

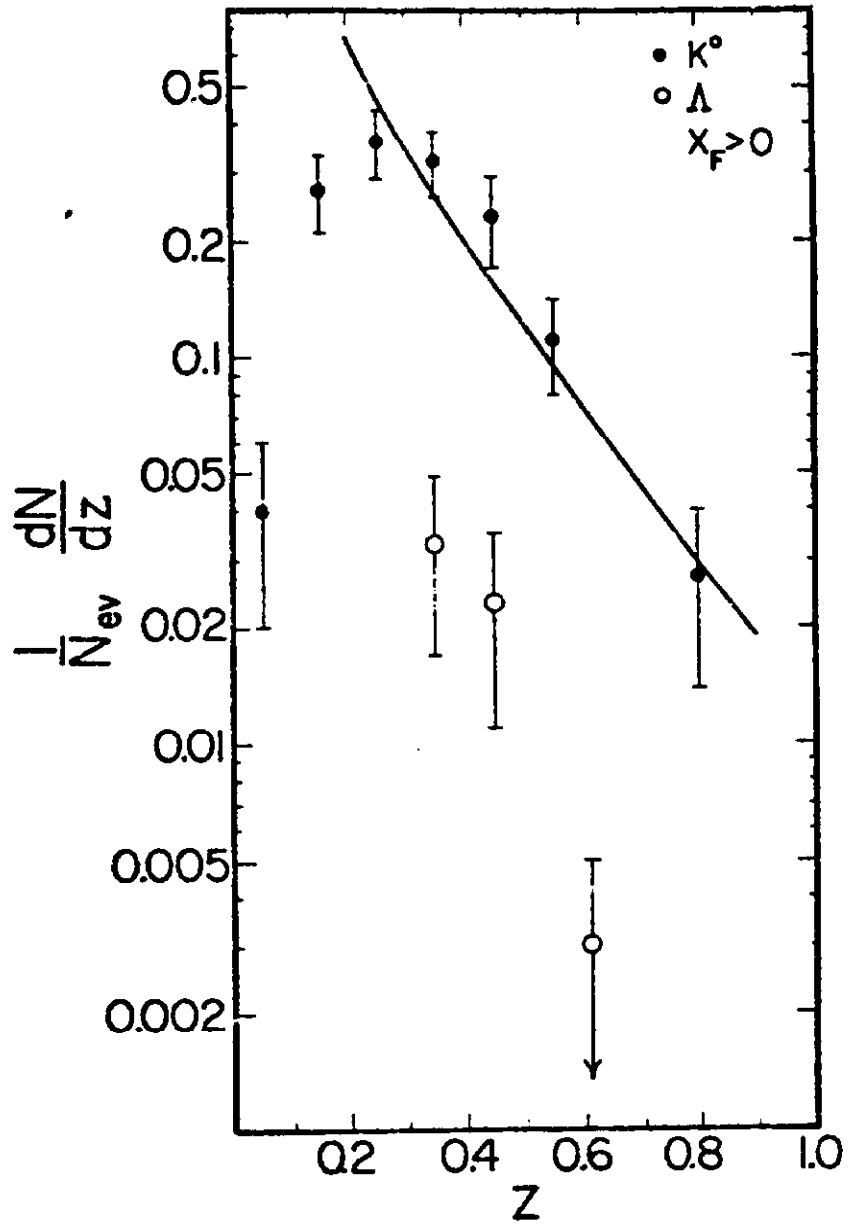


Fig.4

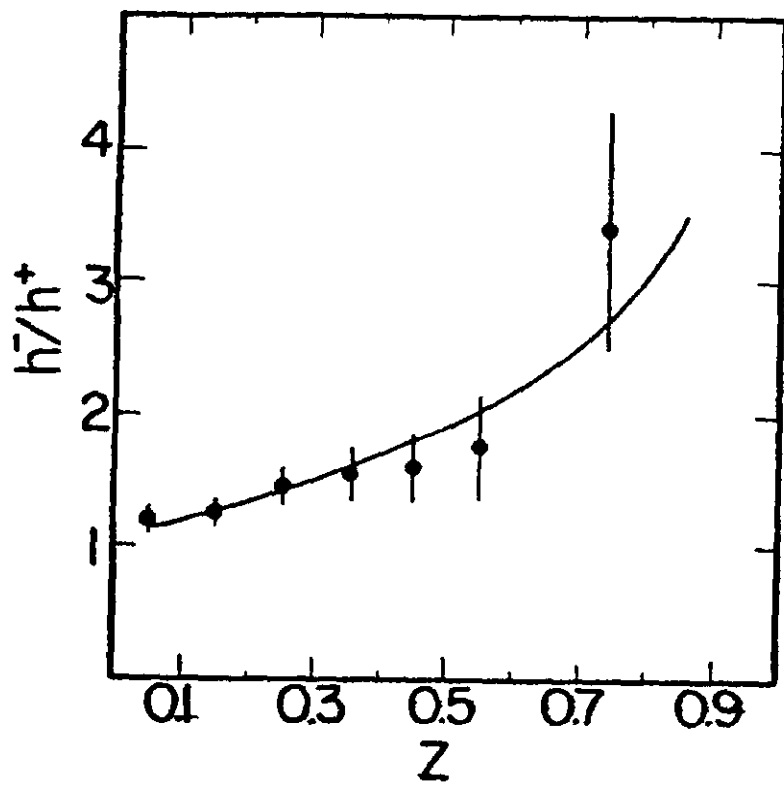


Fig. 5

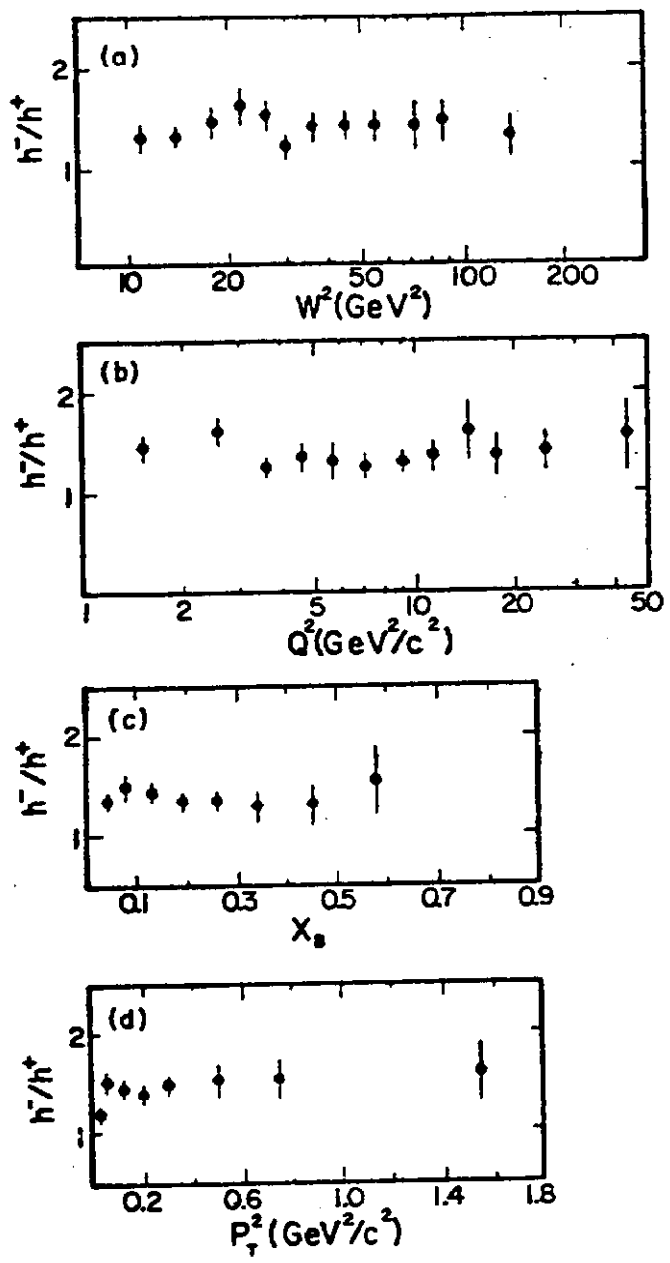


Fig.6

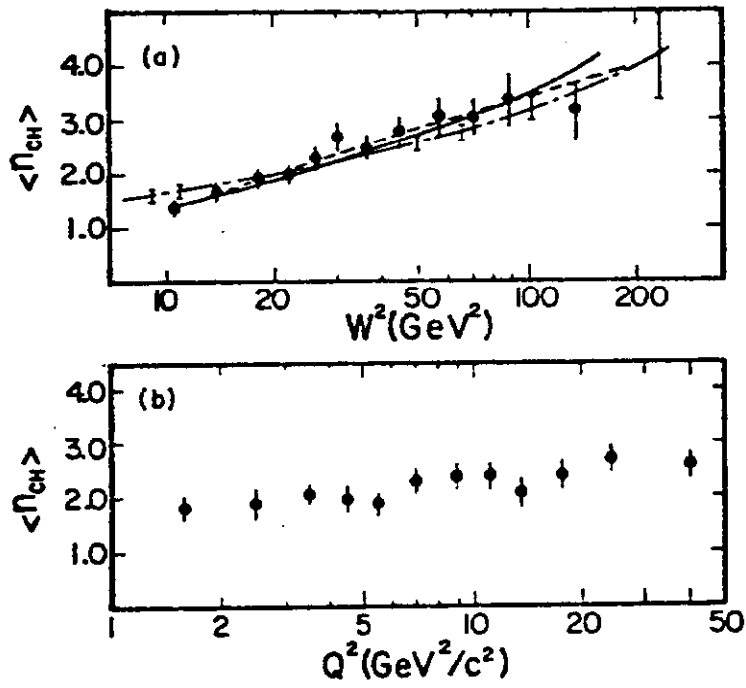


Fig. 7

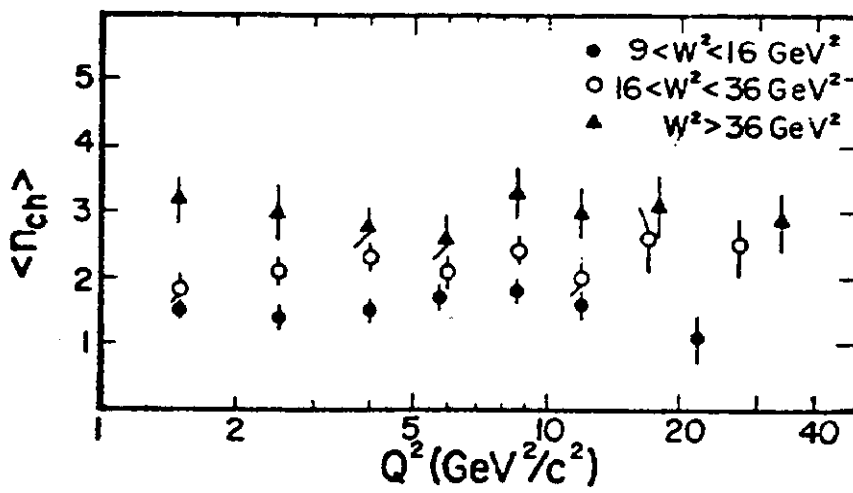


Fig. 8

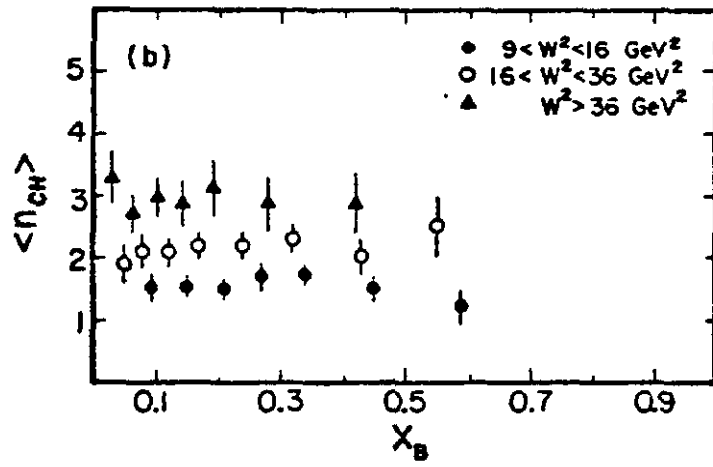
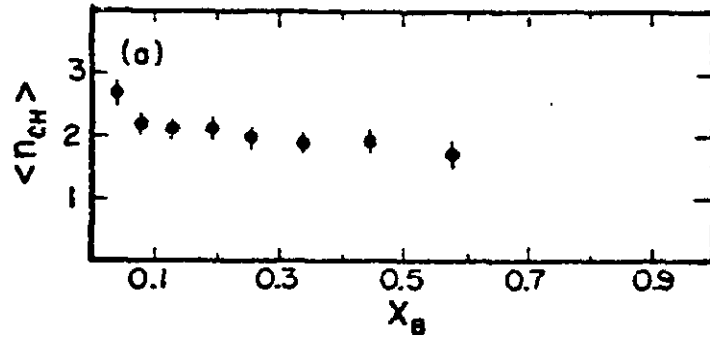


Fig.9

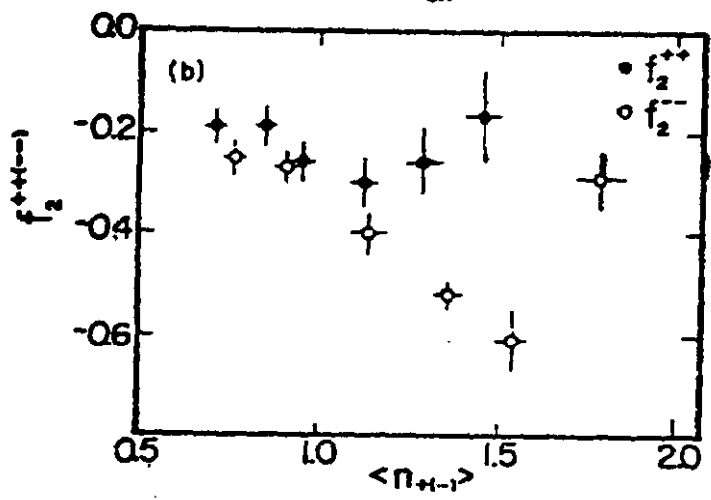
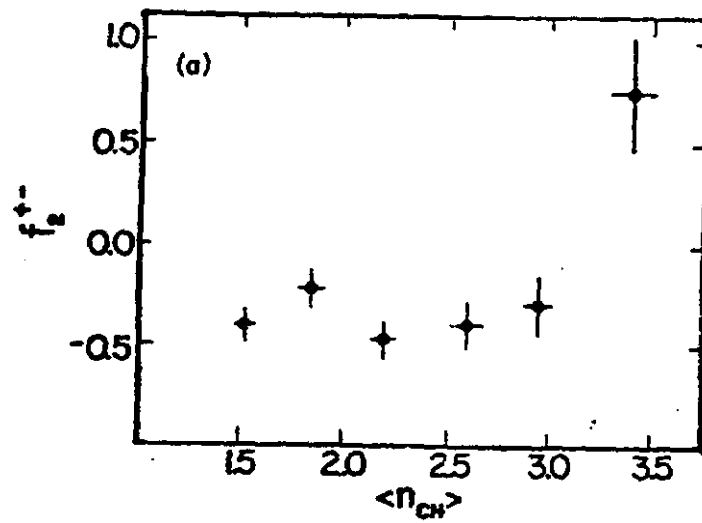


Fig. 10

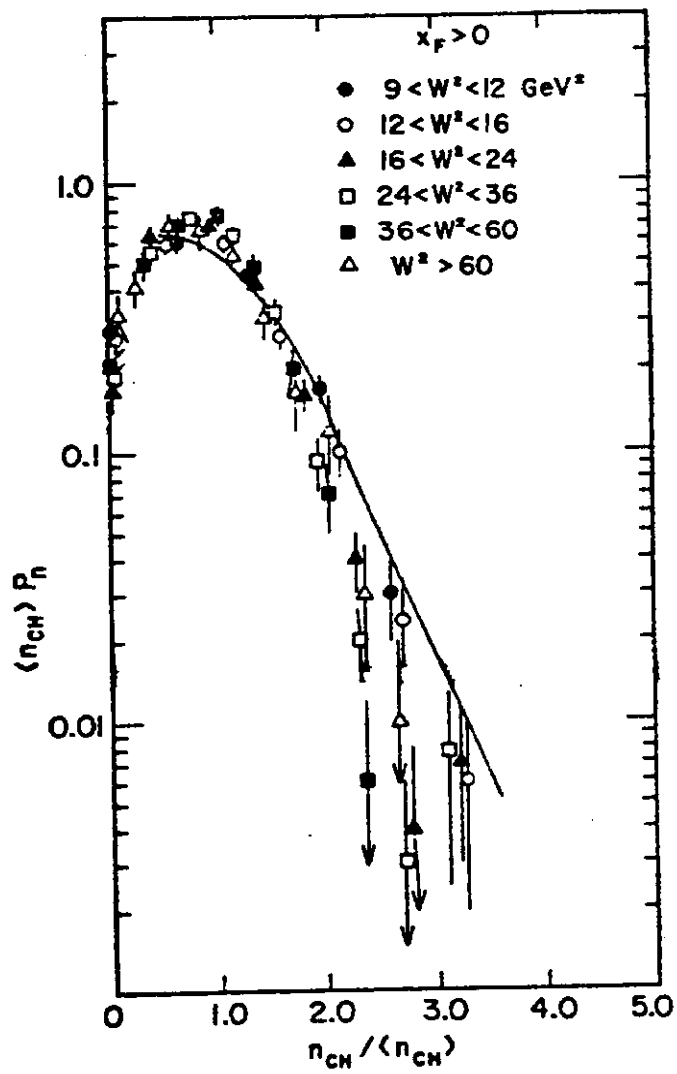


Fig.11

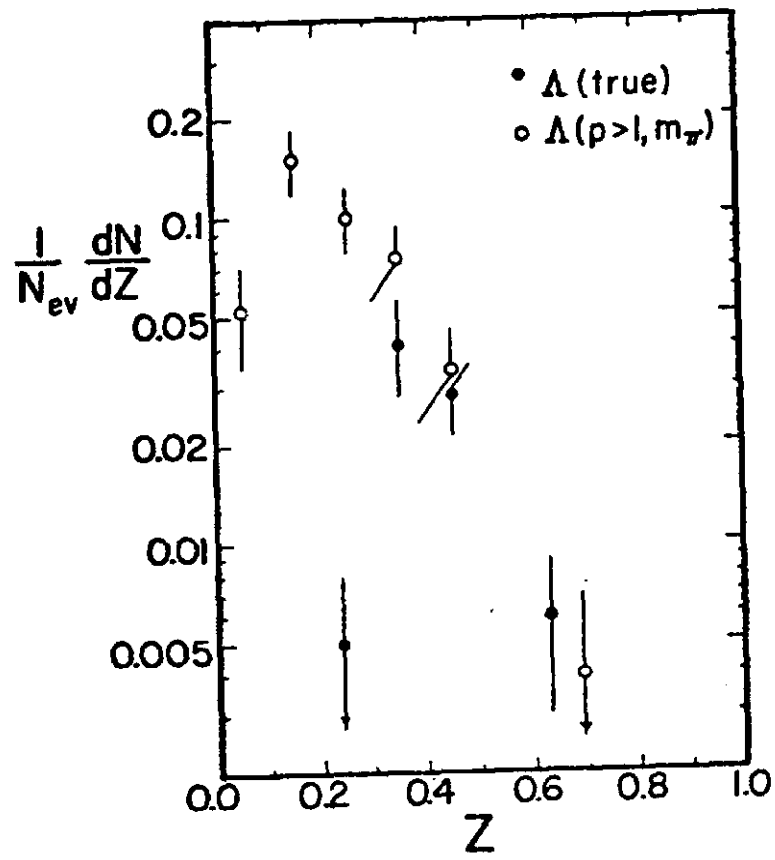


Fig.A1